



¹⁸F-FDG PET-CT for the prediction of mortality in patients with dermatomyositis and without malignant tumors: a pilot study

Yiduo Xu^{1,2,3}, Bing Wang^{1,2}, Feifei Zhang^{1,2}, Min Wu⁴, Dongyan Wang^{1,2}, Xiaoliang Shao^{1,2}, Xiaonan Shao^{1,2}, Jianfeng Wang^{1,2}, Bao Liu^{1,2}, Yunmei Shi^{1,2}, Wenji Yu^{1,2#}, Yuetao Wang^{1,2#^}

¹Department of Nuclear Medicine, The Third Affiliated Hospital of Soochow University, Changzhou, China; ²Institute of Clinical Translation of Nuclear Medicine and Molecular Imaging, Soochow University, Changzhou, China; ³Department of Nuclear Medicine, Affiliated Drum Tower Hospital, Medical School of Nanjing University, Nanjing, China; ⁴Department of Rheumatology, The Third Affiliated Hospital of Soochow University, Changzhou, China

Contributions: (I) Conception and design: Y Xu, W Yu, Y Wang; (II) Administrative support: Y Wang; (III) Provision of study materials or patients: M Wu, D Wang; (IV) Collection and assembly of data: B Wang, F Zhang, Xiaoliang Shao, Xiaonan Shao, J Wang; (V) Data analysis and interpretation: B Liu, Y Shi; (VI) Manuscript writing: All authors; (VII) Final approval of manuscript: All authors.

#These authors contributed equally to this work.

Correspondence to: Yuetao Wang, MD; Wenji Yu, MD. Department of Nuclear Medicine, The Third Affiliated Hospital of Soochow University, No. 185, Juqian Street, Changzhou 213003, China. Email: yuetao-w@163.com; yuwenji0214@163.com.

Background: ¹⁸F-fluorodeoxyglucose positron emission tomography-computed tomography (¹⁸F-FDG PET-CT) is typically used to screen malignancy in patients with dermatomyositis (DM). The aim of this study was to investigate the value of using PET-CT in assessing the prognosis of patients with DM and without malignant tumors.

Methods: A total of 62 patients with DM who underwent ¹⁸F-FDG PET-CT were enrolled in the retrospective cohort study. Clinical data and laboratory indicators were obtained. The muscle max standardized uptake value (SUV_{max}), splenic SUV_{max}, target-to-background ratio (TBR) of the aorta, pulmonary highest value (hv)/SUV_{max}, epicardial fat volume (EFV), and coronary artery calcium (CAC) were measured using ¹⁸F-FDG PET-CT. The follow-up was conducted until March 2021, and the endpoint was death from any cause. Univariable and multivariable Cox regression analyses were used to analyze prognostic factors. The survival curves were produced with the Kaplan-Meier method.

Results: The median duration of follow-up was 36 [interquartile range (IQR), 14–53] months. The survival rates were 85.2% and 73.4% for 1 and 5 years, respectively. A total of 13 (21.0%) patients died during a median follow-up of 7 (IQR, 4–15.5) months. Compared with the survival group, the death group had significantly higher levels of C-reactive protein [CRP; median (IQR), 4.2 (3.0, 6.0) vs. 6.30 (3.7, 22.8)], hypertension [7 (14.3%) vs. 6 (46.2%)], interstitial lung disease [ILD; 26 (53.1%) vs. 12 (92.3%)], positive anti-Ro52 antibody [19 (38.8%) vs. 10 (76.9%)], pulmonary FDG uptake [median (IQR), 1.8 (1.5, 2.9) vs. 3.5 (2.0, 5.8)], CAC [1 (2.0%) vs. 4 (30.8%)], and EFV [median (IQR), 74.1 (44.8, 92.1) vs. 106.5 (75.0, 128.5)] (all P values <0.001). Univariable and multivariable Cox analyses identified high pulmonary FDG uptake [hazard ratio (HR), 7.59; 95% confidence interval (CI), 2.08–27.76; P=0.002] and high EFV (HR, 5.86; 95% CI, 1.77–19.42; P=0.004) as independent risk factors for mortality. The survival rate was significantly lower in patients with the concurrent presence of high pulmonary FDG uptake and high EFV.

Conclusions: Pulmonary FDG uptake and EFV detected with PET-CT were independent risk factors

^ ORCID: 0000-0003-2859-8625.

for death in patients with DM and without malignant tumors. Patients with the concurrent presence of high pulmonary FDG uptake and high EFV had a worse prognosis compared with patients with 1 or neither of these two risk factors. Early treatment should be applied in patients with concurrent presence of high pulmonary FDG uptake and high EFV to improve the survival rate.

Keywords: Dermatomyositis (DM); prognostic factor; interstitial lung disease (ILD); epicardial adipose tissue (EAT); positron emission tomography/computed tomography (PET/CT)

Submitted Oct 27, 2022. Accepted for publication Mar 24, 2023. Published online Mar 30, 2023.

doi: 10.21037/qims-22-1174

View this article at: <https://dx.doi.org/10.21037/qims-22-1174>

Introduction

Dermatomyositis (DM) is a systemic inflammatory disease with an unknown etiology and prognosis that can cause muscle weakness and characteristic skin rashes, while also affecting internal organs, such as the pulmonary and cardiac systems (1). The mortality rate of patients with DM is approximately 3 times that of the general population, and the 5-year survival rate for patients with DM is 60–63% (2). Large population-based cohort studies reported that almost 20–25% of patients with DM have malignant tumors, and DM without malignant tumors is the most common form of DM, accounting for approximately 75% of all cases (3). For these patients, antitumor therapy should be considered first, and their prognosis and life expectancy should be determined by the underlying malignant tumors rather than by DM (4). For patients with DM without malignant tumors, a multidisciplinary approach is recommended. Therefore, it is necessary to screen malignant tumors before treatment to identify risk factors of poor prognosis, which can guide the treatment strategies and improve the survival rate.

¹⁸F-fluorodeoxyglucose positron emission tomography-computed tomography (¹⁸F-FDG PET-CT) is typically used to screen malignancy in patients with DM and can provide a more significant benefit for patients less able to pay out-of-pocket costs than can conventional panels (5,6). Reports have shown that PET-CT may be an effective method in determining whether patients with DM have malignant tumors with high specificity (79–98%) and large ranges in sensitivity (67–94%) (7–10). Other than detecting malignant tumors, ¹⁸F-FDG PET-CT has been recognized as a promising tool in evaluating the activity and severity of interstitial lung disease (ILD) (11,12), which is one of the most important causes of death in patients with DM (13). Furthermore, cardiac involvement occurs in up to 70% of

patients with idiopathic inflammatory myopathy (IIM) and can be lethal (14). As a “one-stop-shop” method, PET-CT is valuable for measuring the indicators of cardiovascular risk, including epicardial fat volume (EFV) and coronary artery calcium (CAC) (15,16).

The aim of this study was to characterize mortality outcomes of patients with DM without malignant tumors and to evaluate the predictors of mortality based on ¹⁸F-FDG PET-CT. We present the following article in accordance with the STROBE reporting checklist (available at <https://qims.amegroups.com/article/view/10.21037/qims-22-1174/rc>).

Methods

Study design and patient selection

We employed a retrospective cohort study design to evaluate the relationship between ¹⁸F-FDG PET-CT findings and mortality outcomes of patients with DM and without malignant tumors. We enrolled patients with DM who underwent ¹⁸F-FDG PET-CT to screen for malignant tumors before treatment in the department of Nuclear Medicine at the Third Affiliated Hospital of Soochow University between July 2013 and July 2020. The data collection was conducted from October 2020 to March 2021. The timing and frequency of the follow-up consultation differed according to patients' general conditions. The inclusion criteria were as follows: (I) the presence of DM diagnosed by experienced rheumatologists according to the 2017 European League Against Rheumatism (EULAR)/American College of Rheumatology (ACR) classification criteria (17) and (II) age >18 and <85 years. The exclusion criteria were as follows: (I) any prior reported or newly diagnosed malignant tumor and

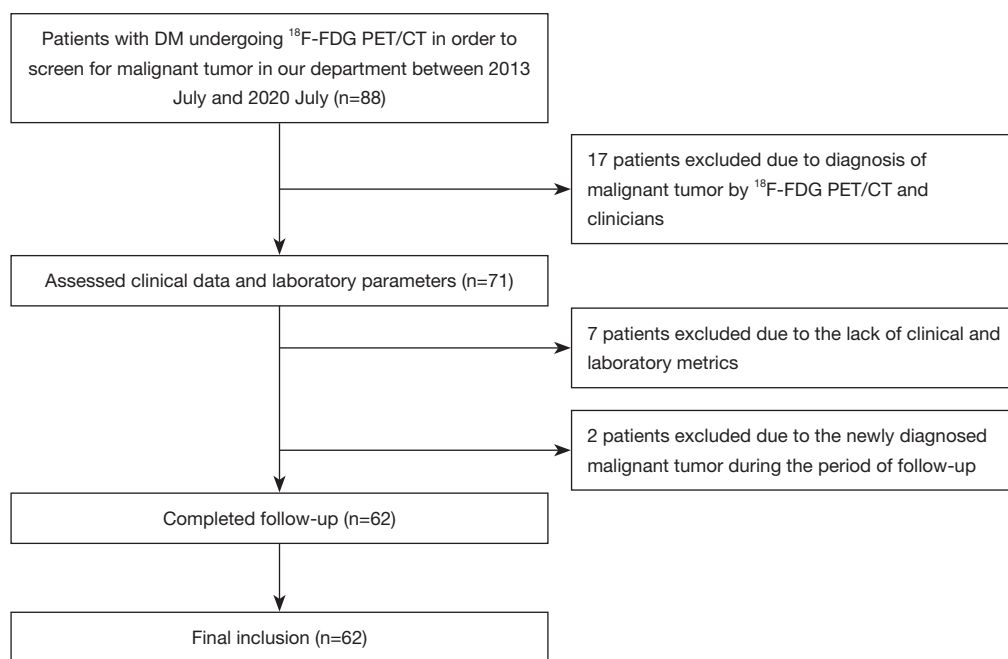


Figure 1 Study flowchart of patient enrollment. DM, dermatomyositis; FDG, fluorodeoxyglucose; PET-CT, positron emission tomography-computed tomography.

(II) a lack of clinical and/or laboratory metrics. Finally, the data of 62 patients with DM were analyzed. *Figure 1* shows the flowchart of the population selection. This study was approved by the Ethics Committee of the Third Affiliated Hospital of Soochow University (No. JD 2020-011) and was conducted according to the Declaration of Helsinki (as revised in 2013). The requirement for informed consent was waived due to the retrospective nature of the study.

Clinical covariates

This study evaluated the patients' demographic and lifestyle characteristics by consulting their medical records at the initial scan and during the follow-up period. Demographic and lifestyle characteristics included age, gender, body mass index (BMI), history of hypertension, diabetes, smoking habits, drinking habits, presence or absence of muscle weakness, and medication. BMI was calculated by dividing the patient's weight (in kg) by their height (in m²) and was used to divide patients into three groups: normal weight (<25 kg/m²), overweight (25–29.9 kg/m²), and obese (≥30 kg/m²) (18). Hypertension was defined as systolic blood pressure ≥140 mmHg, diastolic blood pressure

≥90 mmHg, or the use of antihypertensive drugs. Diabetes was defined as fasting blood glucose ≥126 mg/dL or the use of antidiabetic drugs. ILD was diagnosed through the use of high-resolution CT (HRCT). The most common HRCT abnormalities of ILD are linear opacities, ground-glass attenuation (hyperattenuated areas in which the bronchi and vessels remain visible), reticulation, and peribronchovascular thickening, which are predominantly localized in the lower lobes (19).

Laboratory covariates

Data were gathered by consulting the patient's medical records. Each patient's laboratory indicators were collected within 7 days of the acquisition of the image. These indicators included C-reactive protein (CRP), erythrocyte sedimentation rate (ESR), total cholesterol (TC), high-density lipoprotein cholesterol (HDL-C), low-density lipoprotein cholesterol (LDL-C), triglyceride (TG), lactate dehydrogenase (LDH), creatine kinase (CK), creatine kinase-myocardial band (CK-MB), highly sensitive troponin I (hs-cTnI), antinuclear antibody spectrum, and white blood cell count (WBC).

¹⁸F-FDG PET-CT scanning and analysis

The PET-CT instrument (Biograph mCT 64, 52-ring LSO crystal/64-slice spiral CT, Siemens Healthineers). Prior to the examination, the patients adhered to a fasting period exceeding 8 hours and were administered with ¹⁸F-FDG (Nanjing Jiangyuan Andy Cozhenge Research and Development Co., Ltd., radiochemical pure >95%) via an injection intravenously at a dose of 3.7 MBq/kg. Blood glucose levels were checked (<8 mmol/L) beforehand. Following a period of 60 minutes of rest within a serene and comfortable setting, patients remained in a reclined posture and maintained a consistent respiratory pattern. First, a 64-slice spiral CT scan was performed with a tube current of 35 mA and a tube voltage of 120 kV. After the CT scan, the PET three-dimensional collection was performed. Five to six beds were collected at 2.5 min/bed, and the scanning range was from the top of the skull to the middle and upper part of the femur. Images were evaluated by two experienced nuclear medicine physicians.

First, the muscle FDG uptake was quantified using the maximal standardized uptake value (SUV_{max}) bilaterally by visually focusing on the highest uptake region, away from tendons, in the eight following muscles: deltoideus, biceps brachii, triceps brachii, pectoralis major, psoas major, gluteus group, adductor group, and quadriceps. The muscle SUV_{max} was defined as the average SUV_{max} values of these eight muscles (20).

Second, splenic FDG uptake was measured by placing three regions of interest (ROIs) in orthogonal planes (axial, sagittal, and coronal). For each participant, the splenic SUV_{max} was measured as the average of the three SUV_{max} values (21). Third, the pulmonary FDG uptake was measured by the highest value of the pulmonary SUV_{max} ($h\nu/SUV_{max}$) to represent the severity of ILD in patients with DM. Each lung was split into five representative levels: the origin of the great vessels, the carina, the pulmonary venous confluence, the area halfway between the third and fifth section, and the area 1 cm above the right dome of the diaphragm. These levels represented 10 pulmonary ROIs. The pulmonary $h\nu/SUV_{max}$ was recorded as the highest SUV_{max} of these 10 ROIs (13).

Fourth, to determine the target-to-background ratio (TBR) of the aorta, ROIs were delineated around the aorta in the axial position at intervals of 5 mm along the long axis of the vessel. The mean arterial SUV was obtained by calculating the average of the SUV_{max} values from the serial axial measurements. The venous background SUV was derived from 10 measurements taken in the superior

vena cava. To calculate the TBR, the mean arterial SUV was divided by the mean venous SUV (22). Fifth, epicardial adipose tissue (EAT) was identified as any adipose tissue located within the pericardial sac. EAT was detected by assigning Hounsfield units from -50 to -200 to fat (23). The reader manually traced the pericardial contour with the reconstructed axial slices. The EFV was calculated as the sum of retrospective cohort areas of the fat multiplied by slice thickness. The whole process was completed with syngo software (Siemens Healthineers). Sixth, CAC was identified as a density assessed using a CT scan in the coronary artery surpassing the threshold of 130 Hounsfield units and was quantified using the Agatston method (24).

Follow-up

The follow-up period was defined as the time from diagnosis to either the date of death or March 2021. The endpoint was death from any cause. We confirmed clinical data with medical records or by telephone.

Statistical analysis

We used SPSS 25.0 (IBM Corp.) and MedCalc 18.9.1 (MedCalc Software) for all statistical analyses. The comparisons between the survival and death groups were performed with an independent sample *t*-test for normally distributed continuous variables and the Mann-Whitney test for skewed continuous variables. The chi-squared test and Fisher exact test were applied to compare categorical variables. Receiver operating characteristic (ROC) analysis and the Youden index were performed to determine the optimal cutoff value that maximized the area under the curve (AUC). The AUC value was used to convert continuous variables with no normal range into binary variables. Univariable and multivariable Cox regression analyses were used to analyze prognostic factors of mortality in patients with DM and without malignant tumors. The survival curves were produced with the Kaplan-Meier method, and the log-rank test was used to compare survival rates. A two-sided *P* value <0.05 was considered statistically significant.

Results

Baseline characteristics

Baseline characteristics are shown in *Table 1*. The mean age was 55.4±12.7 years, the majority of patients

Table 1 Baseline characteristics

Characteristics	All patients (n=62)
Demographic parameters	
Age (years), mean ± SD	55.4±12.7
Female gender, n (%)	46 (74.2)
Disease course at initial scan (months), median (IQR)	3.0 (2.0, 12.0)
Time of follow-up (months), median (IQR)	36.0 (14.0, 53.0)
Death, n (%)	13 (21.0)
Clinically amyopathic DM, n (%)	11 (17.5)
Clinical parameters	
BMI (kg/m ²), mean ± SD	22.4±3.2
Muscle weakness, n (%)	11 (17.7)
Hypertension, n (%)	13 (21.0)
Diabetes, n (%)	4 (6.4)
ILD, n (%)	38 (61.3)
Smoker, n (%)	5 (8.1)
Drinker, n (%)	2 (3.2)
Medication at initial scan, n (%)	
NSAIDs	26 (41.9)
GCs	32 (51.6)
ISDs	10 (16.1)
Medication during the follow-up period, n (%)	
ISDs	50 (80.6)
GCs, n (%)	
≤7.5 mg/d	8 (12.9)
>7.5 mg/d	51 (82.3)
Laboratory findings	
CRP (mg/L), median (IQR)	4.3 (3.2, 6.1)
ESR (mm/h), mean ± SD	25.4±16.7
TC (mmol/L), mean ± SD	4.5±1.4
HDL-C (mmol/L), mean ± SD	1.0±0.4
LDL-C (mmol/L), mean ± SD	2.4±0.9
TG (mmol/L), median (IQR)	2.0 (1.6, 2.4)
LDH (μ/L), median (IQR)	305.5 (238.0, 411.9)
CK (μ/L), median (IQR)	116.0 (44.3, 343.8)

Table 1 (continued)**Table 1** (continued)

Characteristics	All patients (n=62)
CK-MB (ng/mL), median (IQR)	3.4 (1.1, 10.3)
WBC (×10 ⁹ /L), median (IQR)	6.2 (4.7, 7.9)
hs-cTnI (ng/mL), median (IQR)	0.005 (0.002, 0.011)
Positive ANA, n (%)	38 (61.3)
Positive anti-Ro60 antibody, n (%)	5 (8.1)
Positive anti-Ro52 antibody, n (%)	29 (46.8)
Positive anti-Jo-1 antibody, n (%)	1 (1.6)
PET-CT quantitative index	
The splenic SUV _{max} , mean ± SD	2.8±0.7
The TBR of the aorta, mean ± SD	1.4±0.2
The pulmonary hv/SUV _{max} , median (IQR)	2.1 (1.5, 2.1)
CAC, n (%)	5 (8.1)
The muscle SUV _{max} , median (IQR)	1.3 (1.1, 1.6)
EFV (cm ³) median (IQR)	76.3 (51.5, 104.0)

SD, standard deviation; IQR, interquartile range; DM, dermatomyositis; BMI, body mass index; ILD, interstitial lung disease; NSAID, nonsteroidal anti-inflammatory drug; GCs, glucocorticoid; ISD, immunosuppressant drugs including cyclophosphamide, methotrexate, tacrolimus, hydroxychloroquine, and mycophenolate mofetil; CRP, C-reactive protein; ESR, erythrocyte sedimentation rate; TC, total cholesterol; HDL-C, high-density lipoprotein cholesterol; LDL-C, low-density lipoprotein cholesterol; TG, triglyceride; LDH, lactate dehydrogenase; CK, creatine kinase; CK-MB, creatine kinase-myocardial band; WBC, white blood cell count; hs-cTnI, highly sensitive troponin I; ANA antinuclear antibody; SUV_{max}, maximum standardized uptake value; TBR, target-to-background ratio; hv, highest value; CAC, coronary artery calcium; EFV, epicardial fat volume.

were female (46/62, 74.2%), and the mean BMI was 22.4±3.2 kg/m². Among the patients with DM, 21% and 6.4% had hypertension and diabetes, respectively. The histopathological examination results of muscular or skin lesions were available in 5 patients (skin biopsy: n=1; muscle biopsy: n=4). There were 6 patients with Gottron papules and 5 patients with a heliotrope rash.

Survival rate and causes of death

The median duration of follow-up was 36 (IQR, 14–53) months. In the overall population, the survival rates were 85.2%

Table 2 Comparison of clinical data between the survival and death group

Characteristics	Survival (n=49)	Death (n=13)	P value
Age (years), mean \pm SD	53.9 \pm 13.2	61.3 \pm 8.5	0.10
Female, n (%)	38 (77.6)	8 (61.5)	0.241
BMI (kg/m ²), mean \pm SD	22.3 \pm 3.2	23.1 \pm 3.1	0.94
Muscle weakness, n (%)	7 (14.3)	4 (30.8)	0.18
Hypertension, n (%)	7 (14.3)	6 (46.2)	0.01
Diabetes, n (%)	3 (6.1)	1 (7.7)	0.84
ILD, n (%)	26 (53.1)	12 (92.3)	0.01
Clinically amyopathic DM, n (%)	6 (12.2)	5 (35.8)	0.04
CRP (mg/L), median (IQR)	4.2 (3.0, 6.0)	6.30 (3.7, 22.8)	0.03
ESR (mm/h), mean \pm SD	24.3 \pm 17.3	29.5 \pm 14.2	0.37
CK (μ /L), median (IQR)	128.0 (46.0, 570.5)	76.0 (32.0, 210.5)	0.14
CK-MB (ng/mL), median (IQR)	4.1 (1.1, 17.9)	3.1 (1.5, 6.4)	0.36
WBC ($\times 10^9$ /L), median (IQR)	6.6 (4.8, 8.0)	5.8 (4.1, 6.6)	0.29
Anti-Ro52 antibody, n (%)	19 (38.8)	10 (76.9)	0.01
The muscle SUV _{max} , median (IQR)	1.4 (1.2, 1.7)	1.1 (1.1, 1.6)	0.34
The splenic SUV _{max} , mean \pm SD	2.8 \pm 0.7	2.8 \pm 0.9	0.17
The TBR of the aorta, mean \pm SD	1.4 \pm 0.2	1.5 \pm 0.2	0.90
The pulmonary hv/SUV _{max} , median (IQR)	1.8 (1.5, 2.9)	3.5 (2.0, 5.8)	0.03
EFV (cm ³), median (IQR)	74.1 (44.8, 92.1)	106.5 (75.0, 128.5)	0.01
CAC, n (%)	1 (2.0)	4 (30.8)	0.001

SD, standard deviation; BMI, body mass index; ILD, interstitial lung disease; DM, dermatomyositis; CRP, C-reactive protein; IQR, interquartile range; ESR, erythrocyte sedimentation rate; CK, creatine kinase; CK-MB, creatine kinase-myocardial band; WBC, white blood cell count; SUV_{max}, maximum standardized uptake value; TBR, the target-to-background ratio; hv, highest value; EFV, epicardial fat volume; CAC, coronary artery calcium.

and 73.4% for 1 and 5 years, respectively. Additionally, 13 patients died during a median follow-up of 7 (IQR, 4–15.5) months, 2 patients died of unknown causes, and 11 died due to disease-specific causes: among the latter, 7 deaths were due to ILD, 2 deaths were due to multiple organ dysfunction caused by infection, and 2 deaths were due to cardiac involvement (1 case of arrhythmia and 1 case of heart failure).

Differences between the survival and death groups

Compared with those in the survival group, the levels of CRP [median (IQR), 4.2 (3.0, 6.0) *vs.* 6.30 (3.7, 22.8); *P*=0.03], pulmonary FDG uptake [median (IQR), 1.8 (1.5, 2.9) *vs.* 3.5 (2.0, 5.8); *P*=0.03], and EFV [median (IQR),

74.1 (44.8, 92.1) *vs.* 106.5 (75.0, 128.5); *P*=0.01] in the death group were significantly higher. Furthermore, hypertension [7 (14.3%) *vs.* 6 (46.2%); *P*=0.01], ILD [26 (53.1%) *vs.* 12 (92.3%); *P*=0.01], positive anti-Ro52 antibody [19 (38.8%) *vs.* 10 (76.9%); *P*=0.01], and CAC [1 (2.0%) *vs.* 4 (30.8%); *P*=0.001] was significantly more common in the death group than in the survival group. No statistically significant differences were observed in other variables (Table 2).

Prognostic risk factors

The cutoff values of the scale variables were determined according to ROC analysis (Table 3) or by reference ranges from the clinical laboratory of the Third Affiliated hospital

Table 3 The cutoff values determined according to ROC analysis

Characteristics	Cutoff value	AUC	Sensitivity (%)	Specificity (%)
Age (years)	>62	0.66	69.23	69.39
Muscle SUV _{max}	≤1.14	0.59	53.85	81.63
Splenic SUV _{max}	≤2.30	0.55	46.15	79.59
TBR of the aorta	>1.24	0.53	100.00	18.37
Pulmonary FDG uptake	>2.68	0.69	76.92	73.47
EFV (cm ³)	>98.42	0.73	69.23	79.59

ROC, receiver operating characteristic; AUC, area under the curve; SUV_{max}, maximum standardized uptake value; TBR, target-to-background ratio; FDG, fluorodeoxyglucose; EFV, epicardial fat volume.

Table 4 Univariable and multivariable Cox regression analyses of prognostic risk factors

Characteristics	Adverse factors	Univariable		Multivariable	
		HR (95% CI)	P value	HR (95% CI)	P value
Age (years)	>62	3.99 (1.23–12.98)	0.02	–	0.74
Hypertension	Positive	4.16 (1.38–12.61)	0.01	–	0.34
ILD	Positive	9.38 (1.22–72.25)	0.03	–	0.19
Anti-Ro52 antibody	Positive	4.43 (1.22–16.14)	0.02	–	0.94
The muscle SUV _{max}	≤1.14	0.26 (0.09–0.78)	0.02	–	0.30
High pulmonary FDG uptake	>2.68	7.76 (2.11–28.54)	0.002	7.59 (2.08–27.76)	0.002
High EFV (cm ³)	>98.42	5.76 (1.76–18.81)	0.004	5.86 (1.77–19.42)	0.004
CACS	>0	6.07 (1.84–10.04)	0.003	–	0.27

HR, hazard ratio; CI, confidence interval; ILD, interstitial lung disease; SUV_{max}, maximum standardized uptake value; FDG, fluorodeoxyglucose; EFV, epicardial fat volume; CACS, coronary artery calcium score.

of Soochow University. The univariable Cox regression analysis showed that an age >62 years [hazard ratio (HR), 3.99; 95% confidence interval (CI), 1.23–12.98; P=0.02], hypertension (HR, 4.16; 95% CI, 1.38–12.61; P=0.01), ILD (HR, 9.38; 95% CI, 1.22–72.25; P=0.03), high pulmonary FDG uptake (the pulmonary hv/SUV_{max} >2.68; HR, 7.76; 95% CI, 2.11–28.54; P=0.002), high EFV (>98.42 cm³; HR, 5.76; 95% CI, 1.76–18.81; P=0.004), CAC (HR, 6.07; 95% CI, 1.84–10.04; P=0.003), muscle SUV_{max} ≤1.14 (HR, 0.26; 95% CI, 0.09–0.78; P=0.02), and positive anti-Ro52 antibody (HR, 4.43; 95% CI, 1.22–16.14; P=0.02) were significantly correlated with the mortality of patients with DM. Multivariable Cox analysis identified that high pulmonary FDG uptake (HR, 7.59; 95% CI, 2.08–27.76; P=0.002) and high EFV (HR, 5.86; 95% CI, 1.77–19.42; P=0.004) were independent risk factors for death (Table 4). According to the log-rank test, patients with high

pulmonary FDG uptake showed lower survival than did those with lower pulmonary FDG uptake (P=0.001; Figure 2A). Survival was lower in patients with a high EFV (P=0.001; Figure 2B) compared to patients with a low EFV. Figure 3 shows the Kaplan–Meier survival curves of high pulmonary FDG uptake and a high EFV. The survival rate was significantly lower in patients with the concurrent presence of high pulmonary FDG uptake and high EFV compared with patients with one or neither of these two risk factors (P<0.001). Representative examples of patients with DM and without malignant tumors are shown in Figure 4.

Discussion

This study had three main findings. First, in patients with DM and without malignant tumors who underwent ¹⁸F-FDG PET-CT, pulmonary FDG uptake and EFV were

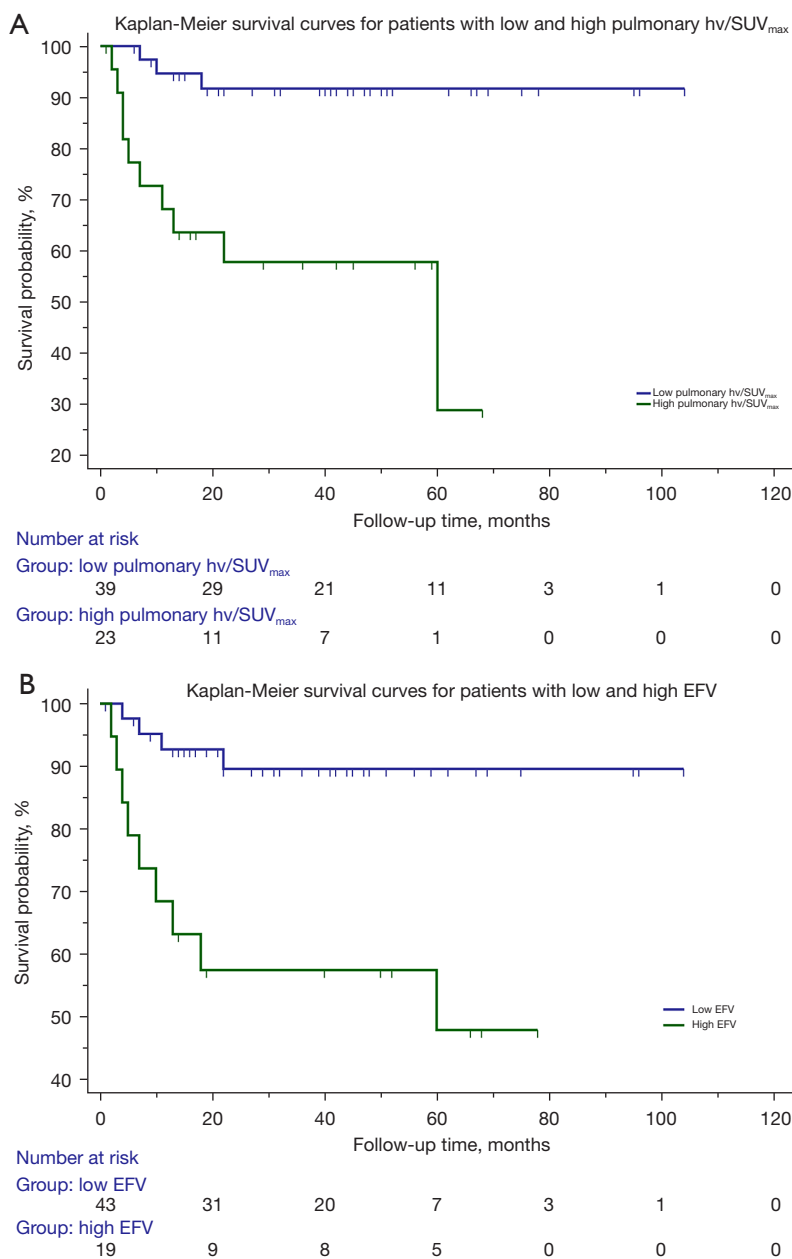


Figure 2 Kaplan-Meier survival curves of patients with DM in the study. (A) Kaplan-Meier survival curves for patients with low and high pulmonary $h\nu/SUV_{max}$ (cutoff value 2.68). (B) Kaplan-Meier survival curves for patients with low and high EFV (cutoff value 98.42 cm^3). $h\nu/SUV_{max}$, highest value of the maximum standardized uptake value; EFV, epicardial fat volume; DM, dermatomyositis.

significantly higher in the death group than in the survival group. Second, a high EFV and high pulmonary FDG uptake were independent risk factors for death in patients with DM and without malignant tumors. Third, patients with the concurrent presence of high pulmonary FDG uptake and a high EFV had worse prognoses.

It has been reported that 20–25% of patients with DM have malignant tumors, and their prognosis and life expectancy are determined by the underlying malignant tumors rather than DM itself (25). Therefore, it is reasonable to compare patients with DM and with and without malignant tumors separately. In the present study,

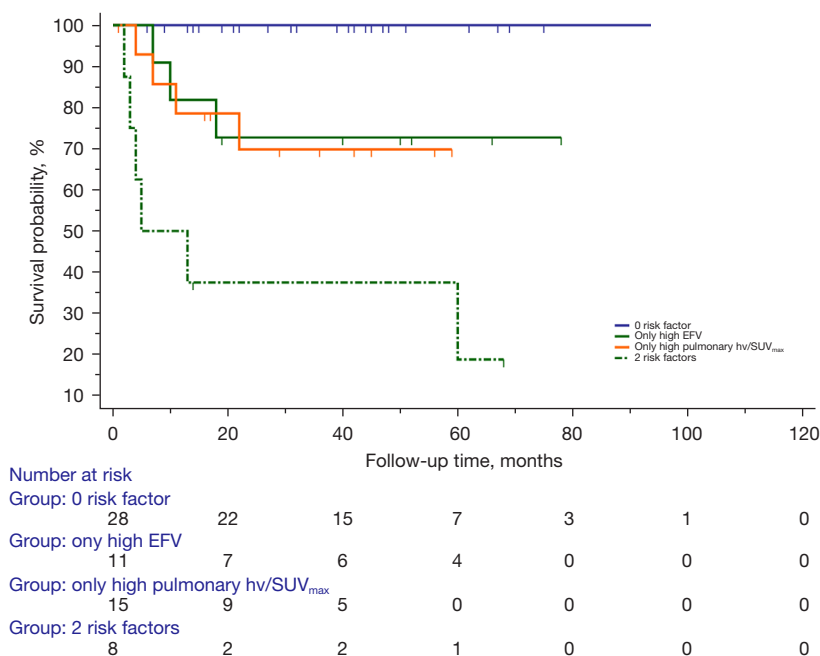


Figure 3 Survival curves of patients with DM based on their numbers of poor prognostic factors. DM, dermatomyositis; EFV, epicardial fat volume; hv/SUV_{max}, highest value of the maximum standardized uptake value.

the presence of malignant tumors was 21.6% (19/88). PET-CT is recommended to detect or exclude malignancy in patients with DM; however, the results of existing studies were controversial. Li *et al.* (26) concluded that PET-CT could identify all 7 cases (18.4%) of malignancies, while Maliha *et al.* (7) showed that PET-CT failed to detect malignancies (including multiple myeloma, squamous cell carcinoma of the skin, and small breast cancer in 3 patients). The failed detection might have occurred because the malignancies were poorly FDG-avid or had a size below the spatial resolution of the camera. Our study focused on the prognosis of patients with DM and without malignant tumors. A recent study reported that survival rates of Chinese patients with DM and without malignant tumors were 81.5% and 76.6% for 1 and 5 years, respectively (27), which are similar to those of our study (85.2% and 73.4%, respectively).

It is widely known that pulmonary involvement is a common cause of mortality in DM, with the most common manifestation being ILD, which affects 10% to 15% of people with DM (28). ILD has been recognized as a predictive parameter of poor prognosis of DM in numerous studies (29). Therefore, the early diagnosis and treatment of ILD are valuable for improving the prognosis

of patients with DM. Clinically, a common method for diagnosing ILD is HRCT. However, a Japanese case report (30) noted that increased pulmonary FDG uptake detected by ¹⁸F-FDG PET-CT occurred 16 days earlier than did the morphological manifestations of ILD as detected on CT, which indicated that ¹⁸F-FDG PET-CT might be more sensitive than HRCT in the early detection of ILD. Similarly, Motegi *et al.* (11) found that the areas of ILD in HRCT also had higher SUV_{max} on ¹⁸F-FDG PET-CT and concluded ¹⁸F-FDG PET-CT findings to be meaningful for the evaluation of the location and the activity of ILD in patients with DM. Furthermore, Li *et al.* (26) showed that a lung mean SUV_{max} cutoff ≥ 2.4 could effectively predict rapidly progressive ILD, which could be life-threatening because of respiratory failure, with a sensitivity of 100% and a specificity of 87% (accuracy 90%).

With reference to Ledoult *et al.* (12), our study used ¹⁸F-FDG PET-CT to detect inflammatory lesions in the patients' lungs, and the pulmonary hv/SUV_{max} was used to represent the severity and activity of ILD in patients with DM. We found that in the multivariable Cox analysis, high pulmonary uptake was an independent risk factor for predicting death while the presence of ILD as detected by HRCT was not. This finding confirmed that compared

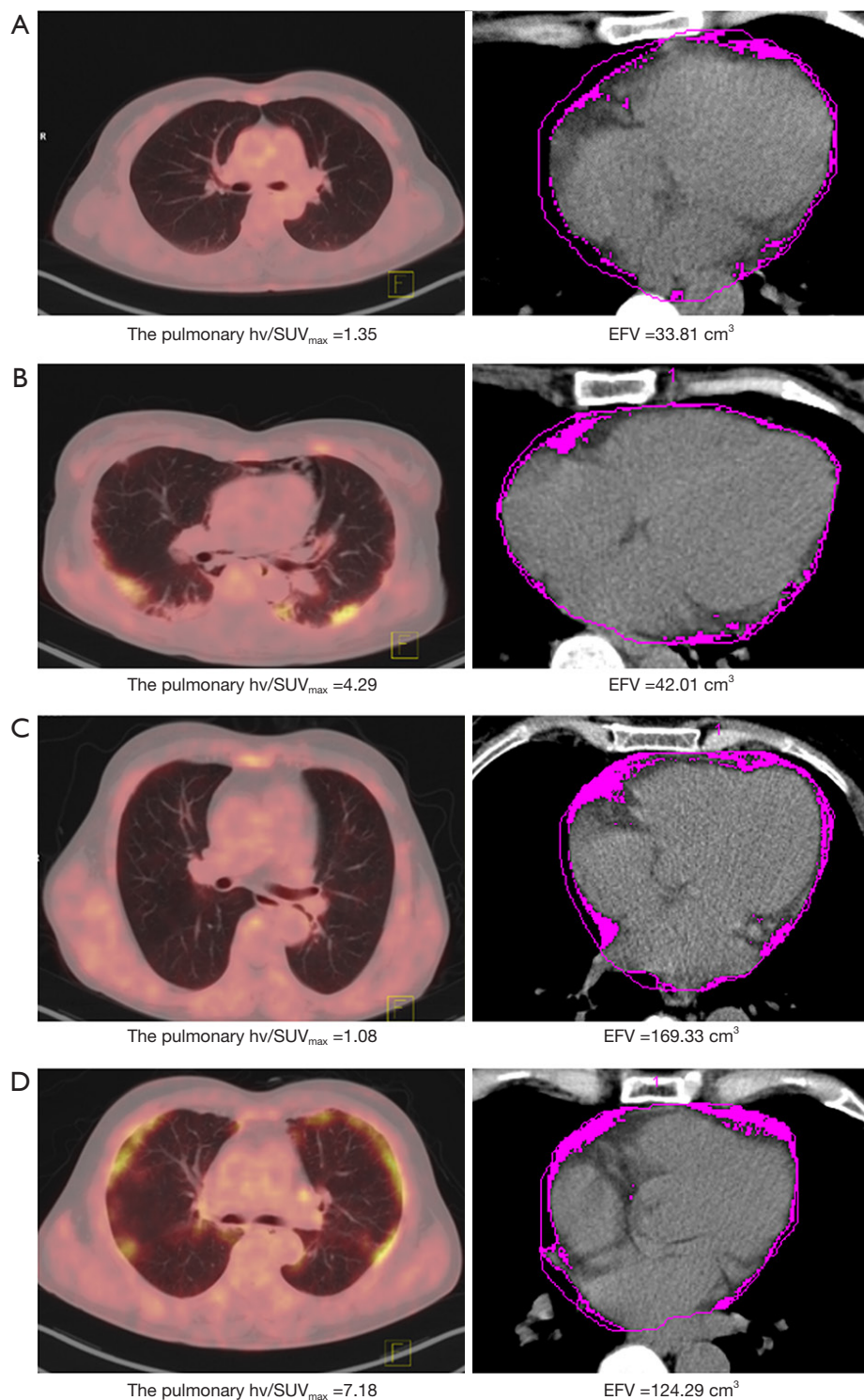


Figure 4 Representative examples of patients with DM with different risk factors. (A) A 43-year-old woman in the survival group was followed up for 95 months and had low pulmonary $h\nu/SUV_{max}$ and low EFV. (B) A 44-year-old woman died within 22 months of diagnosis and had high pulmonary $h\nu/SUV_{max}$ and low EFV. (C) A 65-year-old man died within 18 months of diagnosis and had high EFV and low pulmonary $h\nu/SUV_{max}$. (D) A 64-year-old man died within 13 months of diagnosis and had high pulmonary $h\nu/SUV_{max}$ and high EFV. $h\nu/SUV_{max}$, highest value of the maximum standardized uptake value; EFV, epicardial fat volume; DM, dermatomyositis.

with HRCT, ¹⁸F-FDG PET-CT is uniquely valuable in assessing the severity of ILD and predicting poor prognosis in patients with DM. Furthermore, it is helpful for the early detection of patients with DM who are more likely to experience poor prognoses and require early treatment to improve survival. We hypothesize that this finding may be related to the inflammatory imaging mechanism of ¹⁸F-FDG PET-CT. After the activation of inflammatory cells, a large number of cytokines are released, and the expression of glucose transporters is upregulated, which promotes the uptake of ¹⁸F-FDG by inflammatory cells. The amount of FDG uptake is proportional to the metabolic activity of the cells (31). Since the lung is normally filled with air, for which the metabolic index is zero, the SUV_{max} in the lung is usually negligible. The detection of any inflammatory activity in the lung will differ from the physiological uptake (32). Therefore, ¹⁸F-FDG PET-CT has a unique role in the detection of inflammatory activity in ILD.

Cardiac involvement is considered 1 of the 3 major causes of death in patients with DM other than ILD and malignant tumors (14). At autopsy, subclinical myocardial inflammation is reportedly common and occurs in about one-third of patients with DM (33). EAT, a fat reservoir located between the myocardium and the pericardial visceral layer, has been recognized to be the source of cardiac inflammation and has been used as a new imaging risk marker in metabolic and cardiovascular diseases (16). Several studies developed novel applications for ¹⁸F-FDG PET-CT in cardiovascular involvement caused by inflammation in rheumatic disorders (34,35). However, cardiac ¹⁸F-FDG imaging and EAT ¹⁸F-FDG uptake measurement require patients to complete a low-carbohydrate, high-fat, high-protein diet for 24 hours followed by a minimum of 6 hours fasting before the PET-CT scan in order to inhibit the physiological glucose uptake in the myocardium (36). As we performed a retrospective study, patients enrolled did not perform the above-mentioned preparation before ¹⁸F-FDG PET-CT. Therefore, we only measured EFV and found that high EFV affected the survival rate of patients with DM and without malignant tumors; it may thus be a new important predictor of adverse prognosis in patients with DM.

To the best of our knowledge, this is the first study to analyze the relationship between EFV and mortality in patients with DM and without malignant tumors. Karpouzas *et al.* reported EFV to be associated with a subclinical coronary plaque in rheumatoid arthritis (RA) patients and proposed EAT as a potential marker of subclinical coronary

atherosclerosis and cardiovascular risk in patients with RA (37). We hypothesized that EFV might have a similar effect in patients with DM, as it is also a kind of autoimmune inflammatory disease. Furthermore, EFV was believed to be a risk marker and potential therapeutic target in metabolic syndrome (38), which is more common in IIM than in healthy people (39), and is associated with an increased cardiovascular disease risk (40). Furthermore, Parisi *et al.* (41) believed that statins exert anti-inflammatory effects independent of lipid lowering and found that statin therapy can reduce EAT accumulation and inhibit macrophage-mediated inflammation. However, more in-depth research is needed to determine concretely whether EAT is a potential therapeutic target and to identify the underlying mechanism in DM.

There were several limitations in this study. First, the final sample size was small due to the low prevalence of DM, which may be the reason for the wide 95% CI for EFV and high pulmonary FDG uptake. Additional analyses of large sample sizes or further investigation may be necessary to establish the stability of the model and the validity of the findings. Single-center research might result in biased outcomes. Second, as a retrospective study, the information obtained was limited. We did not analyze other myositis-specific autoantibodies other than anti-Jo-1, such as the anti-melanoma differentiation-associated gene 5 (MDA5) antibody or anti-aminoacyl-transfer RNA synthetase (ARS) antibody. Third, the patients did not prepare for inhibiting physiological glucose uptake in the myocardium (33), and the FDG uptake of the myocardium and EAT were not measured. Fourth, the data lacked evaluations of ILD progress; therefore, the relationship between pulmonary FDG uptake and ILD progress was not analyzed. Further evaluation is required to assess the relationship between pulmonary FDG uptake and ILD. Fifth, the use of ROIs and the calculation of the mean SUV of several muscles was a complex, operator-dependent, and time-consuming feat in daily practice. The binary threshold used for FDG uptake in our investigation was determined through ROC analysis and computation of the Youden index. This approach was necessary because of the absence of universally accepted quantitative benchmarks. In order to ensure consistency across studies, it is recommended that future research assume a standardized, multicenter design with expanded sample sizes, alongside external validation, to identify the optimal threshold. Furthermore, the use of corticosteroids may affect the uptake of FDG. Prospective studies are needed to further evaluate the value of PET

before treatment. Finally, the study focused on patients with DM and did not include patients with polymyositis. In future research, it is necessary to analyze these two subtypes of IIM.

Conclusions

Pulmonary FDG uptake and EFV detected by PET-CT are independent risk factors for death in patients with DM and without malignant tumors. Patients with the concurrent presence of high pulmonary FDG uptake and high EFV had a worse prognosis compared to patients with one or neither of these two risk factors. Patients with concurrent presence of high pulmonary FDG uptake and high EFV require early treatment to improve survival. More in-depth prospective research and exploration of the biological mechanism are warranted.

Acknowledgments

Funding: This research was supported by the National Natural Science Foundation of China [No. 82272031 to principal investigator (PI) Y Wang], the Key Research and Development Program of Jiangsu Province (Social Development; No. BE2021638 to PI Y Wang), and the Science and Technology Project for Youth Talents of Changzhou Health Committee (No. QN202212 to PI W Yu).

Footnote

Reporting Checklist: The authors have completed the STROBE reporting checklist. Available at <https://qims.amegroups.com/article/view/10.21037/qims-22-1174/rc>

Conflicts of Interest: All authors have completed the ICMJE uniform disclosure form (available at <https://qims.amegroups.com/article/view/10.21037/qims-22-1174/coif>). The authors have no conflicts of interest to declare.

Ethical Statement: The authors are accountable for all aspects of the work in ensuring that questions related to the accuracy or integrity of any part of the work are appropriately investigated and resolved. This study was conducted in accordance with the Declaration of Helsinki (as revised in 2013), and the study protocol was approved by the Ethics Committee of the Third Affiliated Hospital of Soochow University (No. JD 2020-011). The requirement for informed consent was waived due to the retrospective

nature of the study.

Open Access Statement: This is an Open Access article distributed in accordance with the Creative Commons Attribution-NonCommercial-NoDerivs 4.0 International License (CC BY-NC-ND 4.0), which permits the non-commercial replication and distribution of the article with the strict proviso that no changes or edits are made and the original work is properly cited (including links to both the formal publication through the relevant DOI and the license). See: <https://creativecommons.org/licenses/by-nc-nd/4.0/>.

References

1. DeWane ME, Waldman R, Lu J. Dermatomyositis: Clinical features and pathogenesis. *J Am Acad Dermatol* 2020;82:267-81.
2. Airio A, Kautiainen H, Hakala M. Prognosis and mortality of polymyositis and dermatomyositis patients. *Clin Rheumatol* 2006;25:234-9.
3. Callen JP. Dermatomyositis. *Lancet* 2000;355:53-7.
4. Waldman R, DeWane ME, Lu J. Dermatomyositis: Diagnosis and treatment. *J Am Acad Dermatol* 2020;82:283-96.
5. Yildiz H, D'abadie P, Gheysens O. The Role of Quantitative and Semi-quantitative [18F]FDG-PET/CT Indices for Evaluating Disease Activity and Management of Patients With Dermatomyositis and Polymyositis. *Front Med (Lausanne)* 2022;9:883727.
6. Kundrick A, Kirby J, Ba D, Leslie D, Olsen N, Foulke G. Positron emission tomography costs less to patients than conventional screening for malignancy in dermatomyositis. *Semin Arthritis Rheum* 2019;49:140-4.
7. Maliha PG, Hudson M, Abikhzer G, Singerman J, Probst S. 18F-FDG PET/CT versus conventional investigations for cancer screening in autoimmune inflammatory myopathy in the era of novel myopathy classifications. *Nucl Med Commun* 2019;40:377-82.
8. Li X, Tan H. Value of (18)F-FDG PET/CT in the detection of occult malignancy in patients with dermatomyositis. *Heliyon* 2020;6:e03707.
9. Trallero-Araguás E, Gil-Vila A, Martínez-Gómez X, Pinal-Fernández I, Alvarado-Cardenas M, Simó-Perdigó M, Selva-O'Callaghan A. Cancer screening in idiopathic inflammatory myopathies: Ten years experience from a single center. *Semin Arthritis Rheum* 2022;53:151940.
10. Selva-O'Callaghan A, Grau JM, Gámez-Cenzano C, Vidaller-Palacín A, Martínez-Gómez X, Trallero-Araguás

- E, Andía-Navarro E, Vilardell-Tarrés M. Conventional cancer screening versus PET/CT in dermatomyositis/polymyositis. *Am J Med* 2010;123:558-62.
11. Motegi SI, Fujiwara C, Sekiguchi A, Hara K, Yamaguchi K, Maeno T, Higuchi T, Hirasawa H, Kodaira S, Tomonaga H, Tsushima Y, Ishikawa O. Clinical value of (18) F-fluorodeoxyglucose positron emission tomography/computed tomography for interstitial lung disease and myositis in patients with dermatomyositis. *J Dermatol* 2019;46:213-8.
 12. Ledoult E, Morelle M, Soussan M, Mékinian A, Béhal H, Sobanski V, Hachulla E, Huglo D, Le Gouellec N, Remy-Jardin M, Baillet C, Launay D. (18)F-FDG positron emission tomography scanning in systemic sclerosis-associated interstitial lung disease: a pilot study. *Arthritis Res Ther* 2021;23:76.
 13. Barba T, Mainbourg S, Nasser M, Lega JC, Cottin V. Lung Diseases in Inflammatory Myopathies. *Semin Respir Crit Care Med* 2019;40:255-70.
 14. Lundberg IE. The heart in dermatomyositis and polymyositis. *Rheumatology (Oxford)* 2006;45 Suppl 4:iv18-21.
 15. Iacobellis G. Local and systemic effects of the multifaceted epicardial adipose tissue depot. *Nat Rev Endocrinol* 2015;11:363-71.
 16. Lehker A, Mukherjee D. Coronary Calcium Risk Score and Cardiovascular Risk. *Curr Vasc Pharmacol* 2021;19:280-4.
 17. Lundberg IE, Tjärnlund A, Bottai M, Werth VP, Pilkington C, de Visser M, et al. 2017 European League Against Rheumatism/American College of Rheumatology Classification Criteria for Adult and Juvenile Idiopathic Inflammatory Myopathies and Their Major Subgroups. *Arthritis Rheumatol* 2017;69:2271-82.
 18. Jinks C, Vohora K, Young J, Handy J, Porcheret M, Jordan KP. Inequalities in primary care management of knee pain and disability in older adults: an observational cohort study. *Rheumatology (Oxford)* 2011;50:1869-78.
 19. Lega JC, Reynaud Q, Belot A, Fabien N, Durieu I, Cottin V. Idiopathic inflammatory myopathies and the lung. *Eur Respir Rev* 2015;24:216-38.
 20. Matuszak J, Blondet C, Hubel  F, Gottenberg JE, Sibilia J, Bund C, Geny B, Namer IJ, Meyer A. Muscle fluorodeoxyglucose uptake assessed by positron emission tomography-computed tomography as a biomarker of inflammatory myopathies disease activity. *Rheumatology (Oxford)* 2019. [Epub ahead of print]. pii: kez040. doi: 10.1093/rheumatology/kez040.
 21. Joseph P, Ishai A, MacNabb M, Abdelbaky A, Lavender ZR, Ruskin J, Nahrendorf M, Tawakol A. Atrial fibrillation is associated with hematopoietic tissue activation and arterial inflammation. *Int J Cardiovasc Imaging* 2016;32:113-9.
 22. Subramanian S, Tawakol A, Burdo TH, Abbara S, Wei J, Vijayakumar J, Corsini E, Abdelbaky A, Zanni MV, Hoffmann U, Williams KC, Lo J, Grinspoon SK. Arterial inflammation in patients with HIV. *JAMA* 2012;308:379-86.
 23. Nagashima K, Okumura Y, Watanabe I, Nakai T, Ohkubo K, Kofune T, Kofune M, Mano H, Sonoda K, Hirayama A. Association between epicardial adipose tissue volumes on 3-dimensional reconstructed CT images and recurrence of atrial fibrillation after catheter ablation. *Circ J* 2011;75:2559-65.
 24. Agatston AS, Janowitz WR, Hildner FJ, Zusmer NR, Viamonte M Jr, Detrano R. Quantification of coronary artery calcium using ultrafast computed tomography. *J Am Coll Cardiol* 1990;15:827-32.
 25. Dank  K, Ponyi A, Constantin T, Borgulya G, Szegedi G. Long-term survival of patients with idiopathic inflammatory myopathies according to clinical features: a longitudinal study of 162 cases. *Medicine (Baltimore)* 2004;83:35-42.
 26. Li Y, Zhou Y, Wang Q. Multiple values of (18)F-FDG PET/CT in idiopathic inflammatory myopathy. *Clin Rheumatol* 2017;36:2297-305.
 27. Yang X, Hao Y, Zhang X, Geng Y, Ji L, Li G, Zhang Z. Mortality of Chinese patients with polymyositis and dermatomyositis. *Clin Rheumatol* 2020;39:1569-79.
 28. Cottin V, Thivolet-B jui F, Reynaud-Gaubert M, Cadranel J, Delaval P, Ternamian PJ, Cordier JF; Groupe d'Etudes et de Recherche sur les Maladies "Orphelines" Pulmonaires. Interstitial lung disease in amyopathic dermatomyositis, dermatomyositis and polymyositis. *Eur Respir J* 2003;22:245-50.
 29. Yamasaki Y, Yamada H, Ohkubo M, Yamasaki M, Azuma K, Ogawa H, Mizushima M, Ozaki S. Longterm survival and associated risk factors in patients with adult-onset idiopathic inflammatory myopathies and amyopathic dermatomyositis: experience in a single institute in Japan. *J Rheumatol* 2011;38:1636-43.
 30. Morita Y, Kuwagata S, Kato N, Tsujimura Y, Mizutani H, Suehiro M, Isono M. ¹⁸F-FDG PET/CT useful for the early detection of rapidly progressive fatal interstitial lung disease in dermatomyositis. *Intern Med* 2012;51:1613-8.
 31. Kumar R, Basu S, Torigian D, Anand V, Zhuang H, Alavi

- A. Role of modern imaging techniques for diagnosis of infection in the era of ^{18}F -fluorodeoxyglucose positron emission tomography. *Clin Microbiol Rev* 2008;21:209-24.
32. Chen DL, Cheriyan J, Chilvers ER, Choudhury G, Coello C, Connell M, et al. Quantification of Lung PET Images: Challenges and Opportunities. *J Nucl Med* 2017;58:201-7.
 33. Lie JT. Cardiac manifestations in polymyositis/dermatomyositis: how to get to heart of the matter. *J Rheumatol* 1995;22:809-11.
 34. Amigues I, Tugcu A, Russo C, Giles JT, Morgenstein R, Zartoshti A, Schulze C, Flores R, Bokhari S, Bathon JM. Myocardial Inflammation, Measured Using ^{18}F -Fluorodeoxyglucose Positron Emission Tomography With Computed Tomography, Is Associated With Disease Activity in Rheumatoid Arthritis. *Arthritis Rheumatol* 2019;71:496-506.
 35. Besenyi Z, Ágoston G, Hemelein R, Bakos A, Nagy FT, Varga A, Kovács L, Pávics L. Detection of myocardial inflammation by ^{18}F -FDG-PET/CT in patients with systemic sclerosis without cardiac symptoms: a pilot study. *Clin Exp Rheumatol* 2019;37 Suppl 119:88-96.
 36. Dorbala S, Di Carli MF, Delbeke D, Abbara S, DePuey EG, Dilsizian V, Forrester J, Janowitz W, Kaufmann PA, Mahmarian J, Moore SC, Stabin MG, Shreve P. SNMMI/ASNC/SCCT guideline for cardiac SPECT/CT and PET/CT 1.0. *J Nucl Med* 2013;54:1485-507.
 37. Karpouzas GA, Rezaeian P, Ormseth SR, Hollan I, Budoff MJ. Epicardial Adipose Tissue Volume As a Marker of Subclinical Coronary Atherosclerosis in Rheumatoid Arthritis. *Arthritis Rheumatol* 2021;73:1412-20.
 38. Iacobellis G, Sharma AM. Epicardial adipose tissue as new cardio-metabolic risk marker and potential therapeutic target in the metabolic syndrome. *Curr Pharm Des* 2007;13:2180-4.
 39. Araujo PAO, Silva MG, Borba EF, Shinjo SK. High prevalence of metabolic syndrome in antisynthetase syndrome. *Clin Exp Rheumatol* 2018;36:241-7.
 40. de Moraes MT, de Souza FH, de Barros TB, Shinjo SK. Analysis of metabolic syndrome in adult dermatomyositis with a focus on cardiovascular disease. *Arthritis Care Res (Hoboken)* 2013;65:793-9.
 41. Parisi V, Petraglia L, D'Esposito V, Cabaro S, Rengo G, Caruso A, Grimaldi MG, Baldascino F, De Bellis A, Vitale D, Formisano R, Ferro A, Paolillo S, Davin L, Lancellotti P, Formisano P, Perrone Filardi P, Ferrara N, Leosco D. Statin therapy modulates thickness and inflammatory profile of human epicardial adipose tissue. *Int J Cardiol* 2019;274:326-30.

Cite this article as: Xu Y, Wang B, Zhang F, Wu M, Wang D, Shao X, Shao X, Wang J, Liu B, Shi Y, Yu W, Wang Y. ^{18}F -FDG PET-CT for the prediction of mortality in patients with dermatomyositis and without malignant tumors: a pilot study. *Quant Imaging Med Surg* 2023;13(6):3522-3535. doi: 10.21037/qims-22-1174